International Journal of Mechatronics and Applied Mechanics
2025, Issue 19, Vol. 1

MECHANICAL CHARACTERISATION OF TELESCOPIC BOOM HINGE POINT OF TRUCK CRANE BASED ON ADAMS

Xin Yunsheng[1], Lv Shuyi[1], Yan Xinyu[1], Lv Ziyue[1], Yuan Yueru[1]*
[1]School of Mechanical Engineering, Taiyuan University of Science and Technology, Taiyuan 030000, P.R.China
Email: xin_yunsheng@tyust.edu.cn

Abstract - Facing more and more complex lifting environment, the truck crane is given higher requirements in terms of operating height and operating stability. In order to ensure the safety of the lifting operation of the truck crane, it is necessary to study the dynamic mechanical characteristics of the telescopic boom of the truck crane in the working process. In this paper, the kinematics model and dynamics model of the truck crane are established based on the vector method, Lagrange's equation and the principle of virtual work. Using Hypermesh and Adams simulation platform, combined with three common working conditions, multi-body dynamics calculations were carried out on the 3D model of the truck crane, and the movement conditions of the truck crane in the three common working conditions and the forces under the movement conditions were obtained. The results show that the load acting on the tail hinge point of the telescopic boom increases as the telescopic boom luffing angle increases. With extension of the telescopic boom length, the load acting on the telescopic boom luffing hinge point and the tail hinge point both increases. Among the three common working conditions, the telescopic boom performs the luffing operation first, and then rotates and extends with better stability. In addition, the peak force at the luffing hinge point during the synchronized movement of the components is 6.98% higher than that during the gradual movement, and the synchronized movement of luffing and extending should be avoided as much as possible. The research results provide a theoretical basis for the scientific formulation of lifting operation programs, and also provide technical support and reference for improving the service life of the truck crane and the safety of the driver.

Keywords: Truck crane, Telescopic boom, Compound motion, Dynamics, Hinge point, Mechanical characterisation.

1. Introduction

Truck cranes are widely used in building construction and equipment installation sites due to their high mobility and flexibility to reach different work sites[1]. However, its complex multi-degree-of-freedom motion characteristics (luffing, rotating, telescoping) and dynamic load coupling effects make lifting operations high-risk engineering activities[3]. The most important component in the lifting operation of a truck crane is the telescopic boom, which is connected to each section of the boom through nesting relationship, and the lifting operation at any point in the three-dimensional space is realised by the luffing, extending and rotating of the telescopic boom[6]. In recent years, the research for the dynamic behaviour of telescopic boom mainly focuses on the establishment of mathematical model, structural optimization, multi-body simulation and experimental validation, but there still exists a vacancy in the research of the load characteristics on the hinge point under the compound motion. And the vibration condition during crane operation is an important factor that affects the crane life and driver's health[8]. Therefore, how to improve the safety, reliability and stability of the structure has attracted the attention of many scholars.

Early studies mostly used analytical methods to construct crane kinematic models. Urbaś et al.[12] built a crane model in the form of articulated coordinates, chi-square transformation matrix and

https://doi.org/10.17683/ijomam/issue19

Lagrangian equation of the second type, and analysed the influence of PID controller settings on the positioning accuracy of the crane. However, such methods are difficult to deal with multi-body coupled nonlinear problems. For this reason, Duong et al.[13] introduced the flexibility of the lanyard and the viscoelastic properties of the arm cylinder to construct the dynamic equations of the telescopic arm considering the coupling of multi-physics fields, but its computational efficiency is limited by the mesh dependence of the finite element method. Xin et al.[14] established the vibration differential equations of movable massive cantilever beam system based on Euler-Bernoulli beam theory, and used the dynamic simulation of the virtual prototype model of the automotive telescopic boom crane in Adams software to verify the effect of the deformation of the flexible body on the force at the hinge point. The floating coordinate system (FFR) method, proposed by Shabana, significantly improves the numerical stability of the dynamical equations under the non-inertial system by embedding the flexible body vibration into the multi-body system through the mode superposition technique, which provides a new paradigm for the modelling of complex working conditions[15]. The above scholars provide useful references for the construction of truck crane models.

The location and mechanical characteristics of the hinge point, as a key node for load transfer, directly affect the structural life. Xu et al.[16] established a mechanical model by studying the working principle of the moving boom system in aerial work trucks and analysed the force of the luffing mechanism, and optimised the hinge points of the luffing mechanism based on particle swarm algorithm and Matlab. Jiao et al.[17] optimised the position of the hinge point of the luffing boom of a gantry crane by using the interior point method based on the optimisation of the penalty function, and verified it by the finite element method. Hu et al.[18] took the hinge point of the girder of the shore bridge as the research object, and analysed the dynamic response mechanism of the whole metal structure of the shore bridge by means of mathematical model and experiment. Tan et al.[19] established a mathematical model for the optimisation of the hinge point position of the lifting mechanism by analysing the mechanical characteristics of the hydraulic cylinder of the moving boom of the lifting mechanism under several extreme working conditions. Wang et al.[20] optimised the position of the hinge point of the fire truck structure to improve the safety performance of the folding boom. In the studies of many scholars, the structure and performance of different working devices have been discussed in depth. Among them, the analyses of the characteristics of the hinge points in the working devices are particularly prominent, which reflect that the hinge points play an important role in the determination of the loads to be borne and their positions in space.

With the progress of CAE technology in recent years, multi-software co-simulation has become a mainstream trend. Xu et al.[21] carried out kinematic analysis and simulation of the folding arm system, discussed the key factors affecting its luffing stability, and improved the luffing stability by adjusting the action parameters of the hydraulic cylinder driving the centre boom in the folding boom system. Yıldırım et al.[22] studied the dynamic characteristics of multi-compartment double bridge crane girders by multibody dynamics analysis with Adams software. Dumitru et al.[23] analysed the impact generated between two objects in a mechanical structure by analytical method, Adams virtual prototype method and Ansys and Abaqus finite element analysis. Shang et al.[24] compared the results of Adams model simulation and MATLAB numerical analysis under the same tracking trajectory and found that the trajectory basically overlaps, which proved the reliability of Adams simulation. Savković et al.[25] achieved a highly accurate measurement of the inter-arm contact force by means of strain gauges and laser vibrometer, and the error of their finite element model was controlled within 5%. Nevertheless, most of the existing studies focus on single motion modes, and there is still a lack of dynamic load test data under compound motion.

The current research has achieved significant results in the field of crane telescopic boom modelling and optimisation. However, the load characteristics of the hinge point under composite motion still face both theoretical and experimental challenges. Aiming at the lack of research on the hinge point of telescopic boom of truck crane under compound motion. In this paper, the kinematics model of the truck crane is constructed based on the vector method, and the dynamics model of the truck crane is established based on the Lagrange equation and the principle of virtual work. The kinematics and dynamics of the telescopic boom under compound motions such as luffing, telescoping and rotating are analysed by the Adams simulation experimental platform, and the loads acting on the hinge points of the telescopic boom and their causes are investigated.

2. Method

Truck cranes are widely used in building construction and equipment installation sites due to their high flexibility, high mobility and applicability to most working conditions. Truck crane consists of truck frame, rotary platform, telescopic boom, luffing hydraulic cylinder, etc. Truck crane is shown in Figure 1.

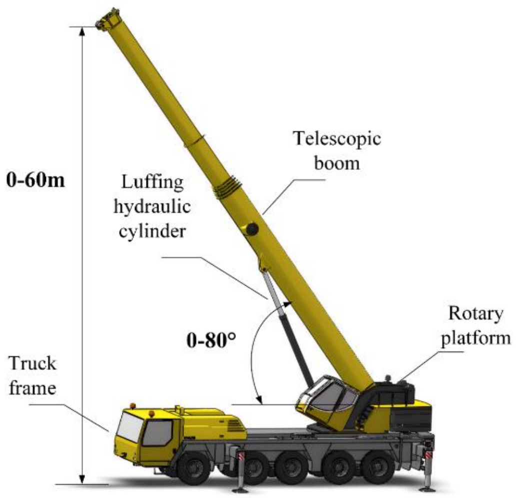

Figure 1:Truck crane

2.1 Kinematic Modeling

The kinematic analysis of a mechanism is the basis for studying the laws of movement of the mechanism, analyzing the forces and improving the performance. The working range of the truck crane is determined by the telescopic boom's extension, rotation and luffing, so the operation process of the telescopic boom is crucial for the truck crane. Generally, the operation process of the truck crane can be divided into six stages: initial, raise, luff, rotation, extension and work. Among them, raising, luffing, rotating and extending are the preparatory processes for the lifting operation.

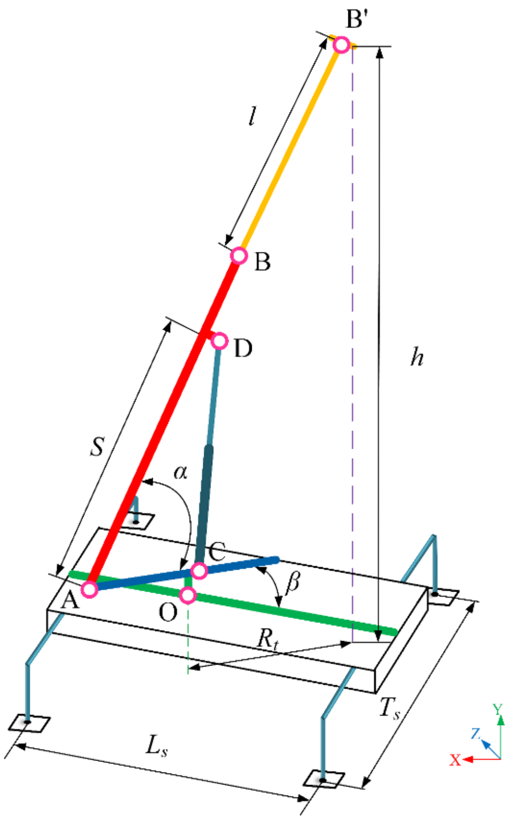

Figure 2: Truck crane sketch

In this paper, the vector method is used to describe the kinematics of the truck crane. The sketch of the truck crane is shown in Figure 2. The model consists of truck frame, rotary platform, telescopic boom, luffing hydraulic cylinder, etc. Point O is the rotating center of the rotary platform. point A is the joint hinge point between the telescopic boom and the rotary platform, and it is also the tail hinge point of the telescopic boom. Point B is the head point of the telescopic boom, point B' is the position after B changes. Point C is the hinge point between the luffing hydraulic cylinder and the rotary platform, point C' is the position after C changes, and D is the hinge point between the luffing hydraulic cylinder and the telescopic boom. The telescopic boom can be extended along the AB direction, the extension length is l , the telescopic boom can be luffed in the plane of BAC with a luffing angle of α , the rotary platform can be rotated around the O point, the rotation Angle is β .

Kinematic expression of the rotary platform, as you can see in equations (1) and (2) below:

$$r_A' = Pr_A \tag{1}$$

$$r_B' = Pr_B \tag{2}$$

Where r_A and r_B represent the position vectors of point A and point B in the global coordinate system at the starting moment, respectively. r_A' and r_B' refer to the new position vectors of r_A and r_B in the global coordinate system after the rotation angle β. P is the coordinate transformation matrix after the rotation angle β, as you can see in equation (3) below:

$$P = \begin{bmatrix} \cos\beta & 0 & -\sin\beta \\ 0 & 1 & 0 \\ \sin\beta & 0 & \cos\beta \end{bmatrix} \tag{3}$$

The velocity equation (4) and acceleration equation (5) of the rotation motion at point B can be obtained by first and second order derivations of equation (2).

$$\dot{r}_B' = \begin{bmatrix} 0 \\ \dot{\beta} \\ 0 \end{bmatrix} \times r_B' \tag{4}$$

$$\ddot{r}_B' = \begin{bmatrix} 0 \\ \ddot{\beta} \\ 0 \end{bmatrix} \times r_B' + \begin{bmatrix} 0 \\ \dot{\beta} \\ 0 \end{bmatrix} \times \dot{r}_B' \tag{5}$$

Kinematic expression of the luffing motion of the telescopic boom, as you can see in equation (6) below.

$$r_B' = Q(r_B - r_A) + r_A \tag{6}$$

where Q is the coordinate transformation matrix after the luffing angle α , obtained from Euler's rotation theorem, as you can see in equation (7) below.

$$Q=\left(2e_0^2-1\right)I+2\left(ee^T+e_0\tilde{e}\right) \tag{7}$$

where I is the unit matrix, $e_0=\cos\frac{\alpha}{2}, e=\frac{r_A}{|r_A|}\times\begin{bmatrix}0\\1\\0\end{bmatrix}\sin\frac{\alpha}{2}, e^T$ is the transpose of e, and $\tilde{e}$ is the skew-symmetric matrix of e.

$$\tilde{e}=\begin{bmatrix}0 & -e_3 & e_2\\ e_3 & 0 & -e_1\\ -e_2 & e_1 & 0\end{bmatrix} \tag{8}$$

The velocity equation (9) and acceleration equation (10) of the luffing motion at point B can be derived from the first and second order of equation (6), respectively.

$$\dot{r}_B^{'}=(r_B-r_A)\times\left(\begin{bmatrix}0\\ \dot{\alpha}\\ 0\end{bmatrix}\times\frac{r_A}{|r_A|}\right) \tag{9}$$

$$\ddot{r}_B^{'}=(r_B-r_A)\times\left(\begin{bmatrix}0\\ \ddot{\alpha}\\ 0\end{bmatrix}\times\frac{r_A}{|r_A|}\right)+\frac{r_A}{|r_A|}\times\dot{r}_B^{'} \tag{10}$$

Kinematic expression of telescopic motion, as you can see in equation (11) below.

$$r_B^{'}=(r_B-r_A)+\frac{(r_B-r_A)}{(r_B-r_A)}l \tag{11}$$

The velocity equation (12) and acceleration equation (13) of the extension motion at point B can be derived from the first and second order of equation (11), respectively.

$$\dot{r}_B^{'}=\frac{(r_B-r_A)}{|r_B-r_A|}\dot{l} \tag{12}$$

$$\ddot{r}_B^{'}=\frac{(r_B-r_A)}{|r_B-r_A|}\ddot{l} \tag{13}$$

If the luffing angle is α, the rotation angle is β and the telescopic boom length l, the three scalars $r_B^{'}$ about the coordinate origin $\left(x_0,y_0,z_0\right)$ can be calculated, and thus the movement state of the telescopic boom can be calculated. The kinematic analysis of the truck crane lays the foundation for dynamic modeling and provides a theoretical basis for the setting of the parameters of the Adams simulation driving function.

2.2 Dynamic Modeling

Dynamic analysis mainly studies the relationship between the motion and the force of the mechanism, which is the basis for mechanical design and structural analysis. Truck crane is a typical heavy-duty construction machinery, in order to accurately study the relationship between the movement changes of each component of truck crane and the load acting on hinge points, it is necessary to carry out dynamic modeling, which can provide an important basis for the optimization of the working performance of the whole machine and the design and research of the control system. It can also guide the Adams setup, such as parameter input, constraint definition, solver selection. Based on Lagrange equation and virtual work principle, dynamic modeling is carried out in this paper.

Based on Newton's second law, the dynamics equation of a single rigid body can be expressed as equation (14) below.

$$\begin{cases}m\ddot{r}-mg-F=0\\ J\cdot\dot{\omega}+\omega\times J\cdot\omega-M=0\end{cases} \tag{14}$$

where, m represents the mass of the rigid body, r represents the vector of the rigid body particle relative to the reference origin, g is the gravitational acceleration, F represents the external force of the rigid body's center of mass, J is the moment of inertia, ω is the angular acceleration, and M is the external moment.

The truck crane system can be regarded as consisting of a single rigid body, and the dynamic equation of the truck crane system based on the principle of virtual work can be expressed as (15) below:

$$\begin{aligned}&\sum_{i=1}^{n}(m_i\ddot{r}_i-m_ig-F_i)\delta\dot{r}\\ &+\sum_{i=1}^{n}(J_i\cdot\dot{\omega}_i+\omega_i\times J_i\cdot\omega_i-M_i)\cdot\delta\omega_i=0\end{aligned} \tag{15}$$

Where, m_i、$\ddot{r}_i$、F_i、J_i、ω_i、$\dot{\omega}_i$ is the mass, centroid acceleration, centroid external force, moment of inertia, angular velocity, angular acceleration, and external torque of the ith rigid body. $\delta\dot{r}_i$ and $\delta\omega$ are its center-of-mass virtual velocity and virtual angular velocity, respectively.

Introducing constraint equation (16).

$$\Phi(q,t)=0 \tag{16}$$

The velocity constraint equation (17) and acceleration constraint equation (18) are derived from the constraint equation (16).

$$\Phi_q\dot{q}+\Phi_t=0 \tag{17}$$

$$\Phi_q\ddot{q}+\dot{\Phi}_q\dot{q}+\dot{\Phi}_t=0 \tag{18}$$

Where Φ_q is the constrained Jacobian matrix.

Since the geometric meaning of the system virtual power equation is that the column vector $M\ddot{q}-F$ is orthogonal to the system virtual velocity $\delta\dot{q}$, equation (19) can be derived.

$$M\ddot{q}-F=\Phi_q^T\lambda \tag{19}$$

λ is a Lagrange multiplier subcolumn vector with the same dimension as the number of constraints.

Note $\xi=-\dot{\Phi}_q\dot{q}-\dot{\Phi}_t$ combines equation (19) with it to get the constrained system dynamics equation (20).

$$\begin{bmatrix} M & \Phi_{\mathbf{q}}^{\mathbf{T}} \\ \Phi_{\mathbf{q}} & 0 \end{bmatrix}\begin{Bmatrix} \ddot{q} \\ -\lambda \end{Bmatrix}=\begin{pmatrix} F \\ \xi \end{pmatrix} \tag{20}$$

A review of the Adams instruction manual reveals that Adams uses differential-algebraic equations to solve the multibody system dynamics, and its numerical implementation is consistent with equation (20) in this paper.

3. Dynamics Calculation

Firstly, a 3D model was built in Solidworks based on the technical parameters of a certain model of truck crane. Secondly, Hypermesh software is used to flexibly process the telescopic boom and generate MNF modal neutral files, which are imported into Adams to replace the rigid telescopic boom of the model. Finally, through the Adams simulation platform to establish a dynamic model that can reflect the movement and dynamic force characteristics of the truck crane, to achieve the kinematic analysis of the lifting operation of the program and dynamics calculation.

3.1 Structure Parameter Setting

A certain model of truck crane is shown in Figure 1, which consists of frame, rotary platform, telescopic boom, luffing hydraulic cylinder, etc.

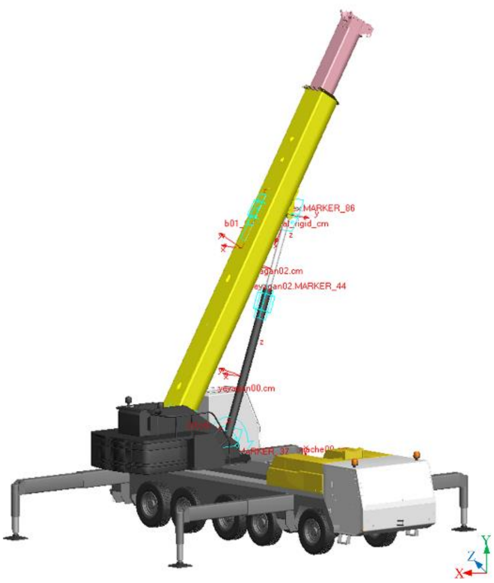

Figure 3: Adams model for truck crane

The number of telescopic boom sections is 7 in total, which is defined as 1th section boom, 2th section boom ...7th section boom respectively from the basic boom, the maximum lifting height is 60m, the maximum angle of luffing is 80°, and the maximum lifting weight is 110 tons, which can satisfy most of the domestic and international engineering operations, the detailed parameters can be referred to Table 1.

Table 1.Parameters of experimental truck crane

Parameter	Symbol	Value
Truck dimension - Length	L	14.5 m
Truck dimension - Width	W	2.75 m
Truck dimension - Height	H	3.95 m
Truck dimension - Wheelbase	W_t	6.8 m
Outrigger span - Longitudinal	L_s	7.5 m
Outrigger span - Transverse	T_s	8.0 m
Distance from points A to D	S	6.9m
Radius of rotation	R_t	3-56m
Lifting height	h	0-60m
Boom self-weight	G_b	8.2t

The model of the truck crane in Adams is shown in Figure 3. Firstly, a global coordinate system (X-horizontal, Z-lateral, Y-vertical) was defined with the ground as the reference and the gravity field was orientated along the negative Z-axis (g = -9.81m/s^2). A local coordinate system is created at each articulation point to ensure that the load components are in the same direction as the dynamical equations. Secondly, the material properties are defined by Adams, in which rigid material (steel) is selected for the frame and the rotating platform, and flexible material is used for the telescopic boom, and the properties of the flexible material, including density (7850 kg/m^3), modulus of elasticity (206 GPa), and Poisson's ratio (0.31). The mass m and moment of inertia J of the telescopic arm in equation (14,15) are obtained.

In addition, there are certain constraints between the components of the truck crane, these constraints reflect the interactions between the components, and all these constraints together constitute the motion process of the truck crane. According to equation (16), the corresponding constraints are set, for example, the rotation of the crane corresponds to the revolute joint, the extension and contraction of the hydraulic cylinder corresponds to the cylindrical joint. By means of the Jacobi matrix Φ_q rank-analysis equations (17,18), it is ensured that the system degrees of freedom are consistent with the number of drivers, avoiding under-constraints and redundant constraints.

Then, according to the kinematics model, the driver function with t , α , β and l as parameter variables is written, so as to realize that each component can move according to the specified requirements. The function Settings are as follows:

The driver function of the telescopic boom luffing:

$$\mathrm{STEP}(time, \ t_1 \ , \alpha_1 \ , \ t_2 \ , \alpha_2)$$

The driver function for the rotation of the rotary platform:

$$\mathrm{STEP}(time, \ t_3 \ , \beta_1 \ , \ t_4 \ , \beta_2)$$

The driver function for the length of the telescopic boom:

$$\mathrm{STEP}(time, \ t_5 \ , l_1 \ , \ t_6 \ , l_2)$$

The extension rate of the telescopic boom, the rotation rate of the rotating platform and the operating capacity of the luffing hydraulic cylinder are strictly referred to the product manual.

Finally, the WSTIFF integral method was set, the simulation step size was 0.01s, the error tolerance was 1e-6, and the maximum number of iterations was 25, to ensure the precision and accuracy of the simulation calculations.

3.2 Working Condition Setting

The actual operation of the truck crane can be divided into five stages: raising, luffing, rotating, extending, and working. These five stages can be combined in different orders, the most critical of which is the order of rotation and luffing. One is to rotate the telescopic boom to the working position first and then carry out the luffing and extending of the telescopic boom (Working condition I), and the other is to carry out the luffing of the telescopic boom first and then rotate it to the working position and extending (Working condition II), and between the two operation programs, there is also a situation in which the luffing and extending work at the same time (Working condition III). In order to investigate the truck crane movement and force under different operation conditions, the above three common working conditions are set up for calculation, and the specific working steps are shown in Table 2.

Table 2. Truck crane operation steps

Step	Working condition I		Working condition II		Working condition III	
1	0-10s	raise	0-10s	raise	0-10s	raise
2	10-32s	rotate	10-32s	rotate	10-80s	extend
3	32-82s	luff	80-130s	luff	80-130s	luff
4	82-502s	extend	10-430s	extend	130-152s	rotate
5	502-547s	work	430-475s	work	152-502s	extend
6					502-547s	work

4. Results and Discussion

In this paper, the dynamics model of the truck crane is calculated by Adams simulation platform, and the movement condition of the truck crane under three common working conditions and the force under the movement state are obtained. According to the calculation results, the kinematics and dynamics are analyzed respectively.

4.1 Kinematic Analysis

In order to better observe the movement of the truck crane, the hinge point D of the crane telescopic boom and the telescopic boom head B are taken as the marking points. The response of the luffing hydraulic cylinder of the truck crane under working condition I is shown in Figure 4a, and the movement trajectory of the telescopic boom is shown in Figure 4b.

In working condition I, the luffing hydraulic cylinder firstly rotates around the hinge point C by a certain angle, and at the same time extends to 1,200mm, completing the raising action, which is convenient for the rotation of the rotary platform and the telescopic boom extending. 10s to 32s the rotary platform rotates 90° to reach the working orientation, in this process, the length and angle of the luffing hydraulic cylinder remain unchanged.

In the 50s time after 32s, the luffing hydraulic cylinder rotates around the hinge point C to 80°, and the luffing hydraulic cylinder extends to 6,000mm, at which time the telescopic boom forms an angle of 80° with the horizontal plane, reaching the maximum luffing angle. After 82s, the telescopic boom extends step by step and reaches the maximum lifting height of 60,000mm in 420s, and finally the rotary platform rotates 180° to simulate the work of lifting.

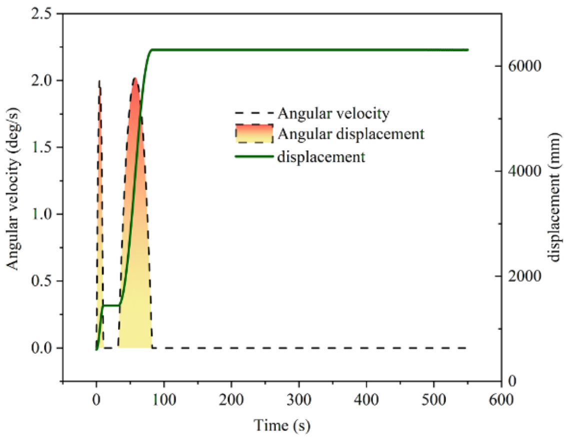

a. Variable amplitude hydraulic cylinder operation

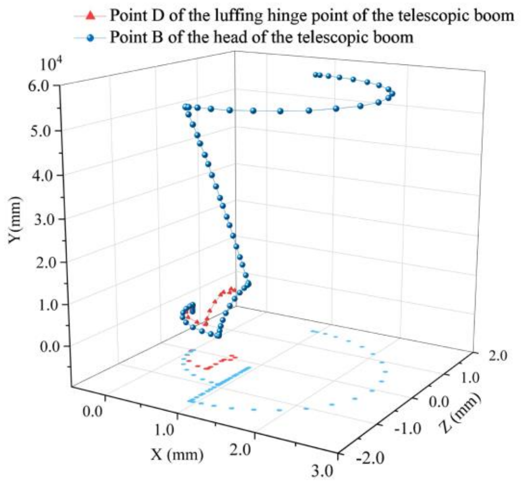

b. Trajectory lines of points B and D

Figure 4: Truck crane movement under working condition I

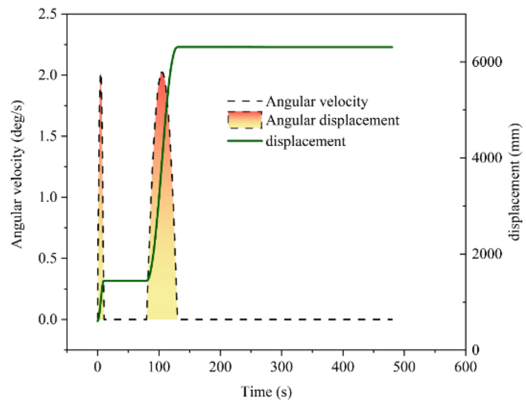

a. Variable amplitude hydraulic cylinder operation

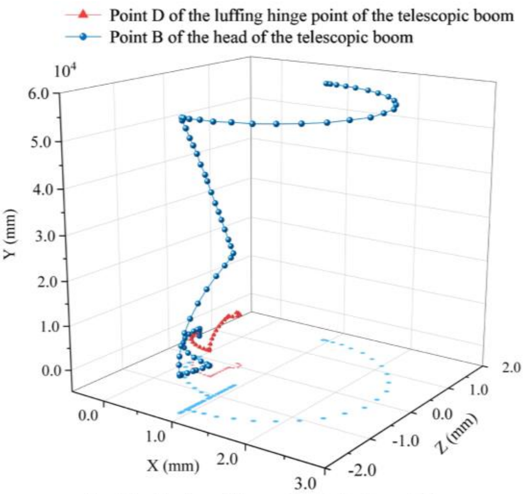

b. Trajectory lines of points B and D

Figure 5: Truck crane movement under working condition II

The response of the luffing hydraulic cylinder of the truck crane under working condition II is shown in Figure 5a, and the movement trajectory of the telescopic boom is shown in Figure 5b. Working condition II is a mixed type of working condition I and III. The luffing hydraulic cylinder firstly rotates around the point C by a certain angle, and at the same time extends to 1,200mm, completing the raising action, which is convenient for the rotation of the rotary platform and the telescopic boom extending. From 10s to 80s the rotary platform rotates 90° with the extension of the telescopic boom to reach the working orientation. After that, the luffing hydraulic cylinder rotates around point C while the telescopic boom extends. Then, the luffing cylinder extends to 6,000mm, the telescopic boom forms an angle of 80° with the horizontal plane to reach the maximum luffing angle. The telescopic boom continues to extend to 60,000mm to reach the maximum lifting height, and finally the rotary platform rotates 180° to simulate the work of lifting.

The response of the luffing hydraulic cylinder of the truck crane under working condition III is shown in Figure 6a, and the movement trajectory of the telescopic boom is shown in Figure 6b. In working condition III, the luffing hydraulic cylinder firstly rotates around the hinge point C by a certain angle, and at the same time extends to 1,200mm, completing the raising action, which is convenient for the rotation of the rotary platform and the telescopic boom extending. From 10s to 80s, the 7th section of the telescopic boom was first extended. In the 50s after 80s, the luffing hydraulic cylinder rotated around point C to 80°, and the length extended to 6,000mm. At this time, the telescopic boom forms an angle of 80° with the horizontal plane, reaching the maximum luffing angle. 130s later, the rotary platform begins to rotate, and rotates by 90°, and in the process, the length and the angle of the luffing hydraulic cylinder remain unchanged. After 152s, the telescopic boom extends step by step and reaches the maximum lifting height of 60,000mm in 350s. Finally, the rotary platform rotates 180° to simulate the work of lifting.

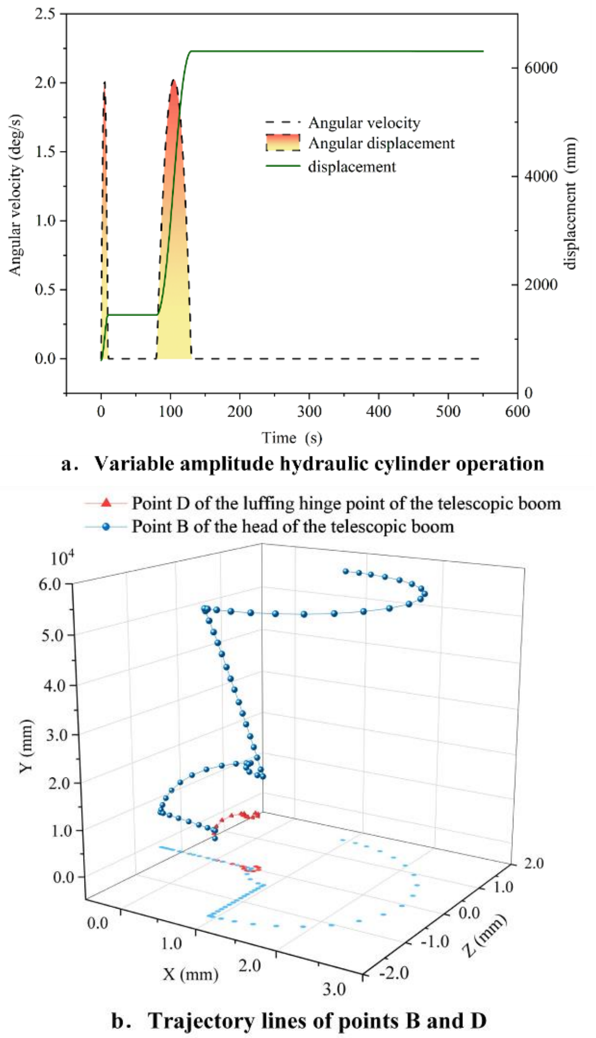

a. Variable amplitude hydraulic cylinder operation

b. Trajectory lines of points B and D

Figure 6: Truck crane movement under working condition III

From the movement of the truck crane, it can be seen that the operation of the luffing hydraulic cylinder of the telescopic boom is consistent with the actual trajectory of the telescopic boom, which can effectively meet the movement requirements of the truck crane under different working conditions.

4.2 Dynamic Analysis

For the telescopic boom of a truck crane, the luffing hinge point D and the tail hinge point A of the telescopic boom are the key positions connecting the rotary platform, the luffing hydraulic cylinder and the telescopic boom, and they are also the two positions where the forces are obvious, so it is necessary to analyze the mechanical characteristics of these two nodes. In this paper, the forces on the luffing hinge point and the tail hinge point of the telescopic boom of a truck crane are extracted with the help of Adams dynamics analysis platform.

The forces on the luffing hinge point and the tail hinge point of the telescopic boom under a single working condition and the forces on the luffing hinge point and the tail hinge point of the telescopic boom under different working conditions are discussed and analyzed respectively.

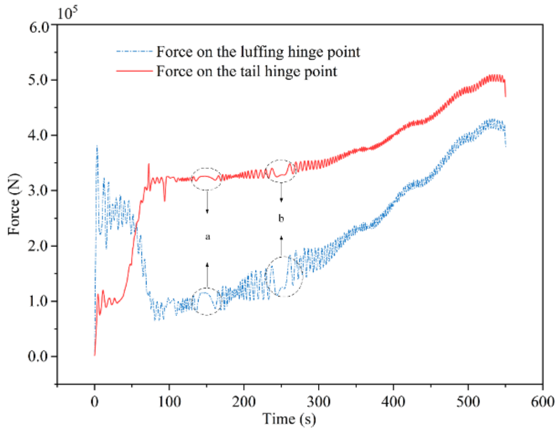

Figure 7: The force on the luffing hinge point and the tail hinge point of the telescopic boom under working condition I.

As can be seen from Figure 7, under working condition I, with the luffing operation of the luffing hydraulic cylinder, the luffing hinge point of the telescopic boom in the early movement of the force is intense, and gradually decreases after reaching the maximum value of 3.8×10^5 N. With the extension of the telescopic boom, the force on the luffing hinge point gradually increases. During the rotating operation of the rotary platform, the force on the luffing hinge point fluctuates within a certain range and has no obvious upward trend. The force on the tail hinge point of the telescopic boom is also obvious at the beginning of the movement, at this time, the force on the tail hinge point of the boom is 1.2×10^5 N, and its peak force is far less than the force on the luffing hinge point of the telescopic boom. With the increase of the angle between the telescopic boom and the horizontal plane, the force at the tail hinge point of the telescopic boom gradually increases, and the force at the tail hinge point of the telescopic boom is gradually higher than that at the luffing hinge point of the telescopic boom. With the extension of the telescopic boom, the force at the tail hinge point of the telescopic boom and the force at the luffing hinge point both increase gradually. Finally, the peak force at the tail hinge point of the telescopic boom reaches 5.1×10^5 N, and the peak force at the luffing hinge point reaches 4.3×10^5 N.

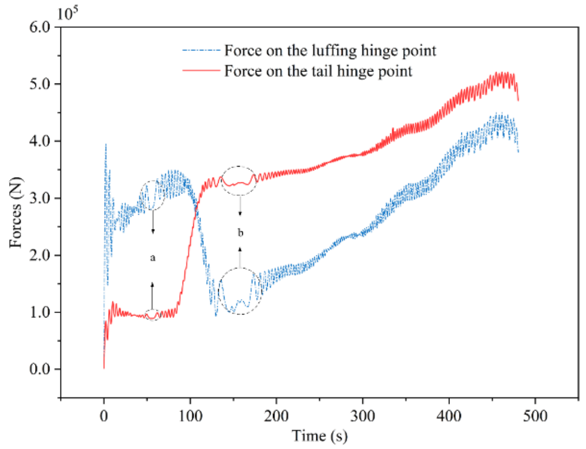

Figure 8: The force on the luffing hinge point and the tail hinge point of the telescopic boom under working condition II

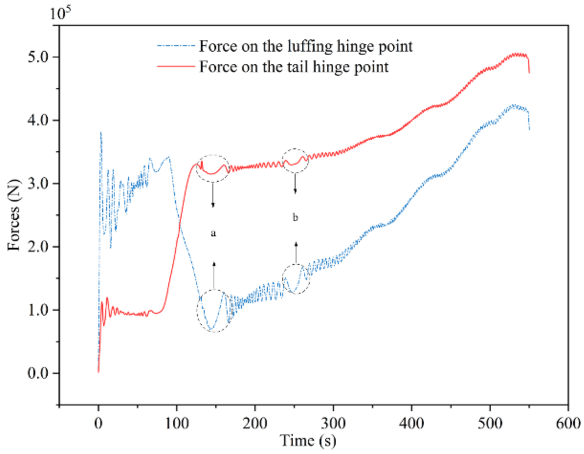

Figure 9: The force on the luffing hinge point and the tail hinge point of the telescopic boom under working condition III.

By observing Figure 8 and Figure 9, it is found that the forces at the luffing hinge point and the tail hinge point of the telescopic boom under working conditions II and III are similar to those at the luffing hinge point and the tail hinge point of the telescopic boom under working condition I. All of them show that the force at the luffing hinge point is higher than that at the tail hinge point at the beginning of the working condition. With the increase of the angle between the telescopic boom and the horizontal plane, the force at the tail hinge point of the telescopic boom is gradually higher than that at the luffing hinge point, and with the extension of the telescopic boom the force at the luffing hinge point and the tail hinge point of the telescopic boom are gradually increased. The obtained results coincide with the operation process of the truck crane, verifying the correctness of the constructed model.

By analysing the force characteristics of the luffing hinge point and the tail hinge point of the telescopic boom. In position a and b of the three working conditions, it is found that when the telescopic boom extends continuously, there will be a small fluctuation for a short period in the two boom alternating stages of the first three booms extension process. That is, there will be a short period of small fluctuations between the fully extended 7th section boom and the initial phase of the 6th section boom, and the fully extended 6th section boom and the initial phase of the 5th section boom. After research and analysis, it is found that this is because there is a kinetic energy response when the new boom starts moving and when the previous boom ends moving, and the two moving realize a coupling. Observations also revealed that this phenomenon was not evident in the latter booms, and the discussion suggested that as the length of the telescopic boom increased giving a mutually balanced force of its own, thus causing this phenomenon to be less pronounced and only showing a trend of rising forces.

Figure 10 shows the force on the luffing hinge point D of the telescopic boom under different working conditions. From Figure 10, it can be found that the trend of the force on the luffing hinge point is basically the same under the three common working conditions, and the force on the luffing hinge point is the process of increasing, then decreasing and then increasing. From Figure 10, it can also be observed that the luffing hinge point has the same force time of 550s in working conditions I and III, and the shortest force time of 480s in working condition II. Although the force time of working condition II is the shortest, its force situation is the most severe, and the force curve of working condition II is always above the force curve of working condition I and working condition III. The peak force on the luffing hinge point in working conditions I and III is 4.3×10^5 N, and the peak force on the luffing hinge point in working condition II is 4.6×10^5 N. The peak force in working condition II is 6.98% higher than the peak force in working conditions I and III.

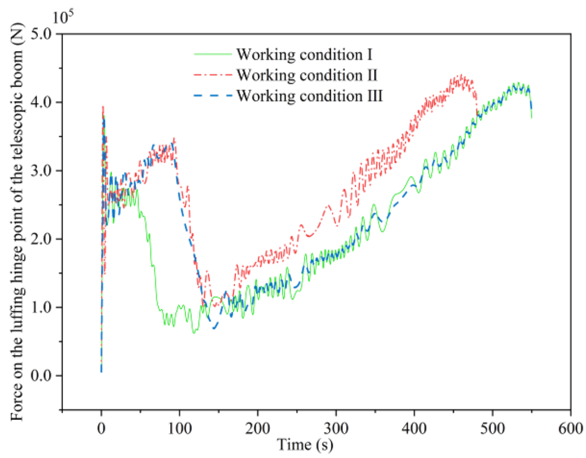

Figure 10: The force on the tail hinge point of the telescopic boom under different working conditions

In the early stage of operation of the truck crane, the force on the luffing hinge point of the telescopic boom in working condition II and working condition III is similar, and the force on the luffing hinge point is always higher than the force on the luffing hinge point in Working Condition I. This is because in working condition II and working condition III, the extension of the telescopic boom gives greater pressure to the luffing hydraulic cylinder, resulting in greater force on the luffing hinge point.

In the late stage of the truck crane operation, the force curves of the luffing hinge points of the telescopic boom in working conditions I and III basically coincide with each other. The force time of the luffing hinge point in working condition I and working condition III is longer than that in working condition II, and the force value is always smaller than that of the luffing hinge point in working condition II.

It can also be observed that the fluctuation range of the force on the luffing hinge point under condition III is within 2.2×10^4 N, which is the smallest fluctuation amplitude among the three conditions. The fluctuation range of the luffing hinge point under operating condition II is within 5.8×10^4 N, which is the largest fluctuation amplitude under the three operating conditions. The analysis found that this is because under the working condition III, the force between the various mechanisms of the truck crane is relatively more balanced, and the overall mechanism is more stable, while under the working condition II, the various mechanisms of the truck crane move synchronously, and the impact and vibration between each other are more obvious, resulting in greater fluctuations.

Figure 11 shows the force on the tail hinge point of the telescopic boom under different working conditions. It can be seen from Figure 11 that the force on the tail hinge point of the telescopic boom under the three working conditions has been in an upward trend, and the force time and force situation at the tail hinge point of the telescopic boom are similar to those at the luffing hinge point of the telescopic boom, with the shortest force time and the most serious force situation under working condition II. At the early stage of the operation of the truck crane, the force on the tail hinge point of the telescopic boom under working condition I rises first, because the telescopic boom under working condition I is the first to reach the maximum luffing angle, so the force on the tail hinge point of the telescopic boom rises first. In the late stage of the operation of the truck crane, the force on the tail hinge point of the telescopic boom is basically the same under working condition I and working condition III.

It is also observed that the fluctuation of the force at the tail hinge point of the telescopic boom is also similar to the fluctuation of the force at the luffing hinge point of the telescopic boom. The fluctuation of the force on the tail hinge point of the telescopic boom under working condition II is the most severe, and the fluctuation range is within 2.4×10^4 N. The fluctuation of the force at the tail hinge point of the telescopic boom in working condition III is the smallest, within 8.9×10^3 N. The fluctuation of the force at the tail hinge point of the telescopic boom under working condition I is within 1.3×10^4 N between working condition II and working condition III.

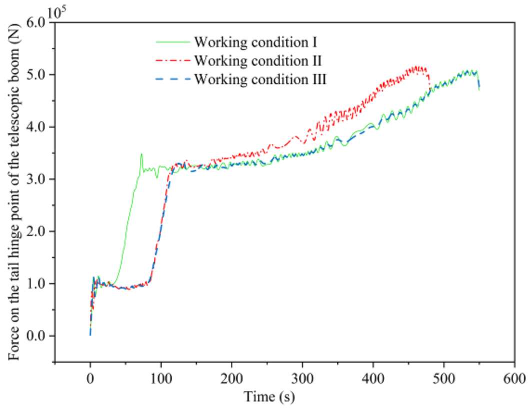

Figure 11: The force on the luffing hinge point of the telescopic boom under different working conditions

Comparing Figure 10 and Figure 11, it can be found that the fluctuation of the force at the luffing point of the telescopic boom under the three working conditions is more severe than the fluctuation of the force at the tail hinge point of the telescopic boom. This is because the number of luffing hydraulic cylinders of this model crane is only one, which is less stable compared to the stout telescopic boom tail, so the fluctuation of the force at the telescopic boom luffing hinge point is more violent than that at the tail hinge point of the telescopic boom.

5. Conclusions

In this paper, based on the vector method, Lagrange's equation and the principle of virtual work, the kinematics model and dynamics model of the truck crane are established, which provide a theoretical reference for analysing the movement process of the truck crane. The calculation of the dynamics model was realised by Adams. The following conclusions are obtained.

(1) When the truck crane carries out the lifting operation, the telescopic boom carries out the luffing operation first and then carries out the rotation and extension of the telescopic boom with better stability. When each mechanism of the truck crane moves synchronously, the mutual impact and vibration between the mechanisms are obviously enhanced,

for example, the telescopic boom carries out luffing operation while the telescopic boom extension operation is carried out at the same time. The peak force of synchronous movement of each component is 6.98% higher than the peak force of gradual movement of each component.

(2) The luffing angle and the length of telescopic boom are important factors affecting the force on the hinge point of telescopic boom. The force on the tail hinge point of the telescopic boom gradually increases with the increase of the luffing angle. At the same time, with the extension of the telescopic boom, the force at the luffing hinge point and the tail hinge point of the telescopic boom will gradually increase.

(3) During the continuous telescopic boom extension operation, there is a kinetic energy response when the starting movement of the new boom and the ending movement of the previous boom. This kinetic energy response affects the stability of the truck crane extension process, and this phenomenon is obvious in the first two booms of the telescopic boom extended.

(4) The telescopic boom force obtained by the calculation method used in this paper coincides with the movement, which can obtain the dynamic force characteristics of the luffing hinge point and tail hinge point of the telescopic boom, and then reveal the dynamic force change rule of the telescopic boom. This not only provides a theoretical basis for the scientific development of lifting operation program, but also provides technical support and reference for improving the service life of the truck crane and the safety of the driver.

However, this study currently only validates the feasibility of the structure at the theoretical level. To realize the engineering application, a real experimental study is still needed. In addition, more comprehensive and detailed data can be obtained by increasing the types of working conditions to provide more reliable support for practical applications.

Acknowledgments

This work was sponsored by the Fund for Shanxi '1331 Project' Key Subject Construction, Shanxi' Science and Technology Platform Project (201805D121005), Postgraduate Innovation Project in Shanxi Province (2024SJ315), Shanxi Province Science and Technology Major Project (20181102002), Applied Basic Research Project of Shanxi Province (201901D211288), Scientific and Technological Innovation Programs of Higher Education Institutions in Shanxi (2019L0649).

Declaration of conflicting interests

The authors declare that they have no known competing financial interests or personal relationships that could have appeared to influence the work reported in this paper.

References

[1] Fu, L., Liu, Y., Fan, Q., & Yin, Y. (2024). Accurate visual localization of the crane boom end. Automation in Construction, Volume 167, Pp: 1-18, 2024. doi: https://doi.org/10.1016/j.autcon.2024.105685

[2] Sadeghi, S., Soltanmohammadlou, N., & Rahnamayiezekavat, P. (2021). A systematic review of scholarly works addressing crane safety requirements. Safety Science, Volume 133, Pp: 1-17, 2021. doi: https://doi.org/10.1016/j.ssci.2020.105002

[3] Raviv, G., Fishbain, B., & Shapira, A. (2017). Analyzing risk factors in crane-related near-miss and accident reports. Safety Science, Volume 91, Pp: 192-205, 2017. doi: https://doi.org/10.1016/j.ssci.2016.08.022

[4] Fang, Y., Cho, Y.K., & Chen, J. (2016). A framework for real-time pro-active safety assistance for mobile crane lifting operations. Automation in Construction, Volume 72, Pp: 367-379, 2024. doi: https://doi.org/10.1016/j.autcon.2016.08.025

[5] Kovalenko, V., Kovalenko, O., Stryzhak, V., Stryzhak, M., & Ruzmetov, A. (2023). Determination of dynamic forces in the metal structure of a tower crane based on the multi-mass model. International Journal of Mechatronics and Applied Mechanics, Volume 14, Pp: 248-256, 2023. doi: https://doi.org/10.17683/ijomam/issue14.29

[6] Trąbka, A. (2014). Dynamics of telescopic cranes with flexible structural components. International Journal of Mechanical Sciences, Volume 88, Pp: 162-174, 2014. doi: https://doi.org/10.1016/j.ijmecsci.2014.07.009

[7] Zheng, Y., & Wang D. (2018). Dynamic Model Studies of Telescopic Crane with a Lifting and Pulling Load Movement. Wireless Personal Communications , Volume 102, Pp: 753-767, 2018. doi: https://doi.org/10.1007/s11277-017-5098-y

[8] Liao, D., Zhu, S., Correia, J.A.F.O., De jesus, A.M.P., & Berto, F. (2020). Recent advances on notch effects in metal fatigue: A review. Fatigue & Fracture of Engineering Materials & Structures, Volume 43, Issue 4 Pp: 637-659, 2020. doi: https://doi.org/10.1111/ffe.13195

[9] Aneziris, O.N., Papazoglou, I.A., Mud, M.L., Damen, M., Kuiper, J., Baksteen, H., Ale, B.J., Bellamy, L.J., Hale, A.R., & Bloemhoff, A. (2008). Towards risk assessment for crane activities. Safety Science, Volume 46, Issue 6 Pp: 872-884, 2008. doi: https://doi.org/10.1016/j.ssci.2007.11.012

[10] Xie, Q., Wen, H., & Wang, Q. (2018). Research and reliability analysis of double bridge crane control system. International Journal of Mechatronics and Applied Mechanics, Issue 4 Pp: 188–195, 2018.

[11] Yao, J., Xing, F., Fu, Y., Qiu, X., Zhou, Z., & Hou, J. (2017). Failure analysis of torsional buckling of all-terrain crane telescopic boom section. Engineering Failure Analysis, Volume 73, Pp: 72-84, 2016. doi: https://doi.org/10.1016/j.engfailanal.2016.12.006

[12] Urbaś, A., Kłosiński, J., & Augustynek, K. (2020). The influence of the PID controller settings on the motion of a truck-mounted crane with a flexible boom and friction in joints. Control Engineering Practice, Volume 103, Pp: 1-13, 2020. doi: https://doi.org/10.1016/j.conengprac.2020.104610

[13] Duong, L.V., & Tuan L.A. (2022). Modeling and observer-based robust controllers for telescopic truck cranes. Mechanism and Machine Theory, Volume 173, Pp: 1-22, 2022. doi: https://doi.org/10.1016/j.mechmachtheory.2022.104869

[14] Xin, Y., Dong, R., & Lv, S. (2023). Dynamic Simulation Analysis of Truck Crane Based on ADAMS. Recent Patents on Mechanical Engineering, Volume 16 Issue 4, Pp: 274–282, 2023. doi: https://doi.org/10.2174/2212797616666230825100256

[15] Shabana, A. A. (2009). Computational Dynamics. John Wiley & Sons, Ltd. ISBN: 9780470686157. https://doi.org/10.1002/9780470686850.

[16] Xu, Y., Xing, B., & Cai, L. (2021). Optimization of hinge point in luffing mechanism of aerial working vehicle based on PSO algorithm., Volume 233, Pp: 1-4, 2021. doi: https://doi.org/10.1051/e3sconf/202123304034

[17] Jiao, Q., Qin, Y., Han, Y., & Gu, J. (2021). Modeling and Optimization of Pulling Point Position of Luffing Jib on Portal Crane. Mathematical Problems in Engineering, Volume 2021, Pp: 1-8, 2021. doi: https://doi.org/10.1155/2021/4627257

[18] Hu, X., Dong, K., Zheng, P., Sun, Z.-W., & Mu, S. (2024). Container quay crane structural dynamic response under trolley traveling. Zhendong Gongcheng Xuebao/Journal of Vibration Engineering, Volume 37, Issue 7, Pp: 1200–1210, 2024. doi: https://doi.org/10.16385/j.cnki.issn.1004-4523.2024.07.012

[19] Tan, J., Liu, Y., Li, W., Wu, D., & Xue, Y. (2024). The optimization of the hinge point position with a 2-DOF planar parallel heavy-duty hoisting mechanism. Journal of Physics: Conference Series, Volume 2862 Issue 1, Pp: 10, 2024. doi: https://doi.org/10.1088/1742-6596/2862/1/012004

[20] Wang, Z., Liu, T., & Guo, T. (2023). Optimization of Key Hinge Points Position of Folding Arm Ascending Platform Fire Truck. Journal of Physics: Conference Series, Volume 2437 Issue 1, Pp: 1-11, 2023. doi: https://doi.org/10.1088/1742-6596/2437/1/012078

[21] Xu, J., Weng, Q., & Wu, J. (2020). Analysis and optimization of folding-boom arm system luffing stability. Ferroelectrics, Volume 562 Issue 1, Pp: 73-84, 2020. doi: https://doi.org/10.1080/00150193.2020.1760595

[22] Yıldırım, Ş., & Esim E. (2022). Investigation of dynamic response of multi- carriages double bridge overhead type crane system subjected to the moving load. Journal of the Brazilian Society of Mechanical Sciences and Engineering, Volume 44 Issue 3, Pp: 1-19, 2022. doi: https://doi.org/10.1007/s40430-022-03419-9

[23] Dumitru, S., Constantin, A., Copilusi, C., & Dumitru, N. (2021). Impact Dynamics Analysis of Mobile Mechanical Systems. Mathematics, Volume 9 Issue 15, Pp: 1-26, 2021. doi: https://doi.org/10.3390/math9151776

[24] Shang, D., Huang, X., Huang, Y. & Zhang, T. (2024). Research on Rigid-flexible Coupling Dynamics of Delta Parallel Robot Based on Kane Equation, Volume 60, Issue 7, Pp: 124-133, 2024. doi: https://doi.org/10.3901/JME.2024.07.124.

[25] Savković, M., Gašić, M., Pavlović, G., Bulatović, R., & Zdravković, N. (2014). Stress analysis in contact zone between the segments of telescopic booms of hydraulic truck cranes. Thin-Walled Structures, Volume 85, Pp: 332-340, 2014. doi: https://doi.org/10.1016/j.tws.2014.09.009